

## MULTIPLE SCATTERING SUPPRESSION IN PLANAR LASER IMAGING OF DENSE SPRAYS BY MEANS OF STRUCTURED ILLUMINATION

Edouard Berrocal\*, Elias Kristensson\*, Mattias Richter\*, Mark Linne\*<sup>o</sup> and Marcus Aldén\*

\* Department of Combustion Physics, Lund Institute of Technology, Box 118, Lund 221 00, Sweden

<sup>o</sup>Sandia National Laboratories, P.O. Box 969, Livermore, California 94551, USA

### ABSTRACT

A novel method to reduce the multiply scattered light contribution in images recorded with planar laser imaging is demonstrated. The technique, **Structured Laser Illumination Planar Imaging (SLIPI)**, is based on spatially modulated excitation light and is here tested within the dense region of a hollow-cone spray. The main idea is to use a laser sheet which is spatially modulated along the vertical direction. By both shifting the spatial phase of the modulation properly and using adequate post image processing of the successive recorded images, it is possible to remove a significant amount of the multiply scattered light detected. In this article, SLIPI is applied for imaging within a typical hollow-cone water spray generated in ambient air at 50 bars injection pressure from a pressure-swirl nozzle. Since this type of spray has a known inner structure, the method can be evaluated, demonstrating that 47 % of the detected light, arising from multiple scattering can be suppressed, resulting in an increase from 61 % to 89 % in image contrast. Such an improvement allows more accurate interpretation and analysis of the near field region of atomizing sprays. The possibility of extracting instantaneous flow motion is also shown here, for a case of a dilute nebulizer. All these results indicate promising applications of the technique in denser turbid media such as air blast atomizer or diesel sprays.

### INTRODUCTION

At present, the study of sprays and other two-phase flows is mainly performed using laser imaging techniques. These modern optical diagnostics have numerous applications as well in the combustion engineering areas as in the medical field. Depending on their source/detector arrangement, imaging can be performed using the back, forward or side scattering detection. One of the most popular side scattering detection methods, employed for flow visualization, is planar laser imaging. This approach offers both qualitative and quantitative two-dimensional resolved measurements. Thanks to these advantages and depending on the physical quantities measured, various planar laser imaging diagnostics applied to spray characterization have been developed during the past three decades: Particle Image Velocimetry [1], Particle Tracking Velocimetry [2], Planar Laser Induced Fluorescence [3], Planar Drop Sizing [4] (or Laser Sheet Dropsizing [5]) and droplet lasing [6], to mention a few. Although these techniques use different properties of light scattering and approaches, they are all based on the single scattering approximation, assuming that the detected photons have experienced only one scattering event prior to arrival at the detector. This assumption remains valid when the number density of particles is low and when the total photon path length within the probed medium is short. However, within optically thick media (e.g. the dense spray region) a large amount of photons are multiply scattered and the single scattering assumption is no longer valid. In this case, the multiple scattering blurs and attenuates the recorded images, introducing significant uncertainties in the detected optical signal [7]. This multiple scattering contribution is particularly important in planar imaging, due to the use of both a relatively wide source of light and a large detection

acceptance angle of the collection optics. Even if various procedures have been employed in order to correct and compensate for the light extinction (attenuation) along the laser path, using iterative procedure of the Beer-Lambert law [8] or illumination from both sides of the probed volume [9], no technique has been proposed, so far, for the correction of the light being multiply scattered from the laser sheet to the detector. In this study we investigate the possibility to suppress this multiply scattered light by using **Structured Laser Illumination Planar Imaging (SLIPI)**. This technique is inspired by **Structured Illumination Microscopy (SIM)** (demonstrated by Neil *et. al.* [10]) and is implemented here in a planar Mie scattering imaging configuration. The medium probed is a hollow-cone water spray, operating within the atomization regime. Particular attention is given to the dense spray region where the conventional method is largely hampered by errors due to multiple scattering. In parallel to these measurements, another droplet flow created this time by a nebulizer is probed. This flow, more dilute and slower than the hollow-cone spray, has been employed in order to demonstrate the capability of the technique when freezing the flow motion. The study of the spray was based on recording an average of 50 single SLIPI images; whereas, only "single shot" SLIPI images were considered for the case of the nebulizer.

The article is structured as follows: In the first section the principle of the technique is explained with some theoretical considerations. The second section describes the experimental set-up. The third section highlights the main results, for both the hollow-cone spray and the nebulizer. Finally a discussion regarding the efficiency of the method in removing the multiply scattered light contribution from multiple scattering is provided.

## THEORY

Structured illumination is based on intensity modulation, in the spatial domain, of the excitation light. Such a modulation can be created by projecting a grating onto the sample of interest. In microscopy, structured illumination can be used to remove out-of-focus photons, which may cause blurring effects on the resulting image. Similar unwanted effects can be seen in a planar laser measurement, but in this case caused by multiply scattered light. By using intensity modulated excitation light it is possible to suppress such light in the post image processing. Here, the main idea is that photons which have experienced several scattering events within the sample will lose the modulation information (of the excitation light), while singly scattered photons will not. Illuminating a sinusoidal grating results in a fringe pattern  $s(x,y)$  (see Fig.1) of the form

$$s(x,y) = 1 + m \cdot \cos(2\pi \nu y + \Phi_0) \quad (1)$$

where  $m$  denotes the modulation depth,  $\nu$  is the spatial frequency,  $\Phi_0$  is an arbitrary spatial phase while  $x$  and  $y$  is the coordinate axes. Such an illumination leads to an image  $I(x,y)$  [9] according to

$$I(x,y) = I_C + I_S \cdot \cos(2\pi \nu y + \Phi_0) \quad (2)$$

This collected light  $I(x,y)$  can be divided into two different images, denoted  $I_C$  and  $I_S$  (see Fig.2) The first image  $I_C$  contains all light, i.e. both singly and multiply scattered light, and is referred to as the *conventional* image later in the text. This image describes how the illuminated sample would look if there was no modulation. The second image  $I_S$  contains only singly scattered photons and corresponds to the SLIPI image. The cosine term describes the superimposed fringe pattern, which must be removed in order to obtain the true SLIPI image  $I_S$ . This can be achieved by recording three images,  $I_1$ ,  $I_2$  and  $I_3$ , with the relative spatial phases  $\Phi_0 = 0$ ,  $2\pi/3$  and  $4\pi/3$ .

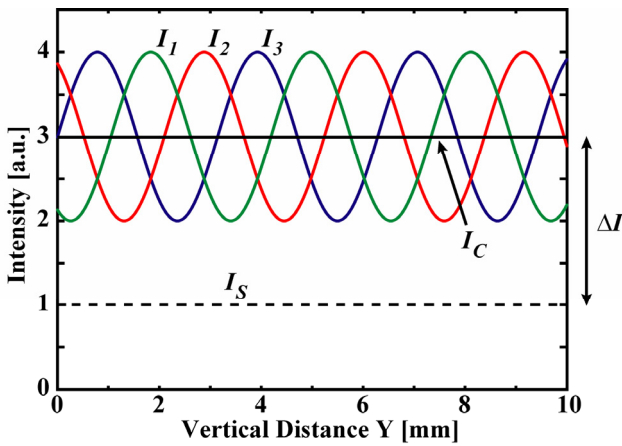


**Fig.1.** Example of spatially modulated signal: When an intensity offset  $\Delta I$  is superimposed on the modulation, the conventional signal is affected by  $\Delta I$  while the SLIPI signal is able to suppress this offset. Note that in practical cases the induced offset, which is linear in this graph, varies with position depending on the optical density and the scattering process involved within the probed medium.

When changing the phase, the intensity modulation is moved along the vertical  $y$ -axis and a change of  $2\pi/3$  will shift the modulation a third of a period. However, the multiply scattered light, which is superimposed on the intensity modulation, is unaffected by this shift. By calculating the pairwise difference between the three recorded images, the multiply scattered light, together with the unwanted intensity modulation, is removed. This is described by the following equation [8]:

$$I_S = \frac{\sqrt{2}}{3} \cdot [(I_1 - I_2)^2 + (I_1 - I_3)^2 + (I_2 - I_3)^2]^{1/2} \quad (3)$$

and

$$I_C = \frac{I_1 + I_2 + I_3}{3} \quad (4)$$

Thus, both the conventional and the SLIPI image can be extracted from the three spatially modulated images. Note that for an increase of the optical depth, i.e. a denser sample, the modulation depth  $m$  decreases since fewer photons are directly scattered to the camera. At large optical depths almost all light is multiply scattered. In this case the modulation depth, together with the intensity of the SLIPI image, will be reduced to zero.

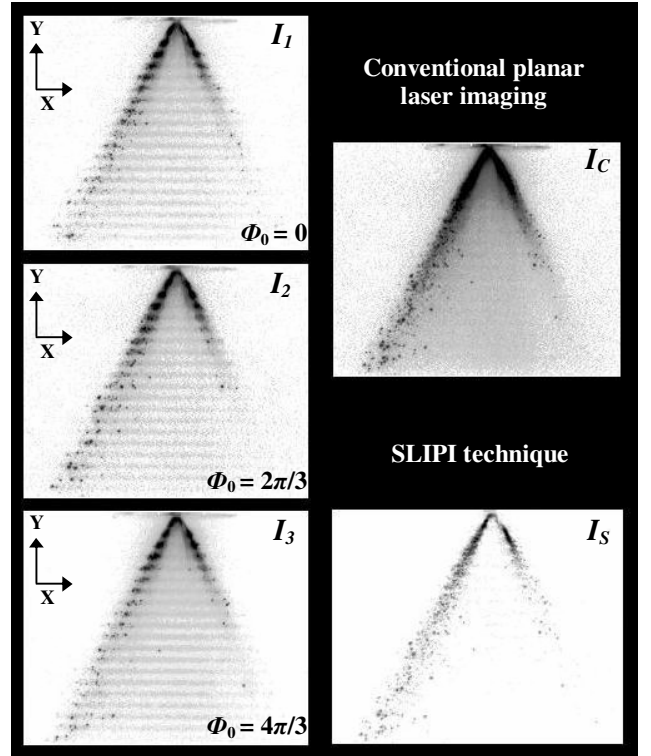


**Fig.2.** Illustration of the SLIPI technique: 3 successive images are taken by illuminating different part of the spray after shifting the spatial modulation one third of a period.

When summing up the images, the conventional planar imaging is obtained, whereas, when extracting the absolute value of the differences between the images, a new image is formed without most of the multiply scattered light.

## EXPERIMENTAL SET-UP

The spray was illuminated from a coherent laser source at a wavelength of 532 nm. The laser sheet was formed by associating a negative cylindrical lens and a positive spherical lens positioned at a respective distance equal to the sum of their focal distance. The resulting laser sheet dimension in the middle of the spray was  $\sim 1$  mm wide and 25 mm high. The images  $I_1$ ,  $I_2$  and  $I_3$  were respectively recorded from three successive laser pulses (10 ns time-width), which were generated from two Nd:YAG lasers; one running in a single pulsed mode, while the second one was running in a double pulsed mode. All beams were then recombined to spatially overlap. The grid pattern was shifted a third of a period between the three pulses by using a rotating plane-parallel quartz plate. The individual beams entered the glass plate at different angles shifting the beams and the modulation pattern vertically. The spatial frequency of the grid was 10 LP/mm producing a spatial modulation period of  $\sim 1$  mm after magnification.

The detection system employed was a multi frame camera, consisting in three 12-bit intensified CCDs of 960 X 1280 pixels. Each CCD array imaged an individual pulse (P1, P2 or P3) and each pixel corresponded to an imaged area of 25  $\mu\text{m}$  square.

The time separation  $\Delta t$  between pulses is governed by both the rotation speed of the quartz plate and the spatial frequency of the grating. Note that  $\Delta t$  is in this experiment neither limited by the laser system nor by the multi-frame camera. The time separation is, here, equal to 55  $\mu\text{s}$  resulting in a total time delay of 110  $\mu\text{s}$ . For this delay, a displacement from pixel to pixel can be noticed only if the velocity motion is larger than 25 cm/s. Due to the high flow motion of the spray  $I_S$  and  $I_C$  were extracted from 50 averaged images. However, for the nebuliser, "single shot" SLIPI images could be recorded.

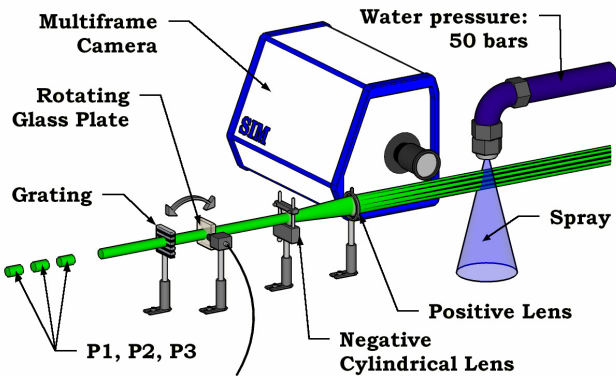


Fig.3. Illustration of the experimental set-up.

The nozzle employed in the experiment was a *Danfoss* 1910 pressure-swirl nozzle type, producing a hollow-cone with nominal  $56^\circ$  cone angle. This type of nozzle is commonly used to create water mist for extinguishing fires. Here, water was sprayed at an injection pressure of 50 bars into an atmospheric pressure optical chamber. At 3 mm below the nozzle tip, 26.5% of light transmission was measured, corresponding to an optical depth of 1.33. PDA measurements can be performed at such optical depth and an average droplet size of  $\sim 20$   $\mu\text{m}$  in diameter has been previously measured [11].

## RESULTS AND DISCUSSION

### a) Application to a hollow-cone spray

Two different experimental configurations are presented Fig.4. On the left side, measurements were performed in the central axis of the spray whereas on the right side the planar illumination was  $\sim 5$  mm off-axis (behind) the nozzle centre. Figure 4 (a) and (b) corresponds to the conventional images, while the SLIPI images are shown in Fig.4 (c) and (d) respectively. In all images the laser sheet entered the spray on the left side of the spray.

In the centre of the spray, no droplets were generated from the pressure swirl nozzle, creating an inner conical structure. The intensity of the signal recorded from this region should, in principle, be equal to zero. However, since light is multiply scattered within the spray, photons falsely appear as though originating from the centre of the spray. This contribution from multiple scattering can be observed in image (a) and it is equal to 24 % at  $X = 17.3$  mm (as seen in the intensity profile of  $I_C$  given in (e)).

Similarly, in the off-axis case, no light should be detected near the nozzle tip region. However, it can clearly be seen in (b) how multiple scattering affects the resulting image, in which non-illuminated parts of the spray are visible.

Multiply scattered photons give rise to a global blurring effect in each of the three successive images  $I_1$ ,  $I_2$  and  $I_3$ . On the contrary, the singly scattered photons which carry the structural information will differ from image to image due to the induced phase shift. The global blurring can then be removed by implementing Eq.(3). This process extracts mainly the singly scattered photons and resulting in a significant increase in image contrast, as seen in the SLIPI images (c) and (d).

In order to quantify the effectiveness of the method, a cross section, defined by the white dashed box (10 mm X 5 mm), is presented at the bottom of Fig.4. These intensity profiles are normalized with the cross section of the conventional image. Two symmetrical peaks, resulting from the hollow-cone structure of the spray, are observed in (e). The 24 % intensity signal previously observed for  $I_C$  at  $X = 17.3$  mm, is reduced in  $I_S$  to only 3 %. This 21 % decrease in light intensity arising from multiple scattering is highlighted in the bottom graph, where the signal difference  $\Delta I$  between the conventional  $I_C$  and the SLIPI  $I_S$  profiles is given. It can be seen that the maximum  $\Delta I$  reaches 47 % at  $X = 15.7$  mm, where  $I_C$  is close to its peak value. This distance  $X$  corresponds to the region where primary and secondary break-up processes occur and where the number density of droplets is the highest.

An estimation of the image improvement is performed by evaluating the image contrast according to

$$C = \frac{I_{\max} - I_{\min}}{I_{\max} + I_{\min}} \quad (5)$$

where  $I_{\max}$  and  $I_{\min}$  are indicated in Fig. 5. For this set of averaged images, the contrast increases from  $C = 61$  % in the conventional image, to  $C = 89$  % for the SLIPI image.

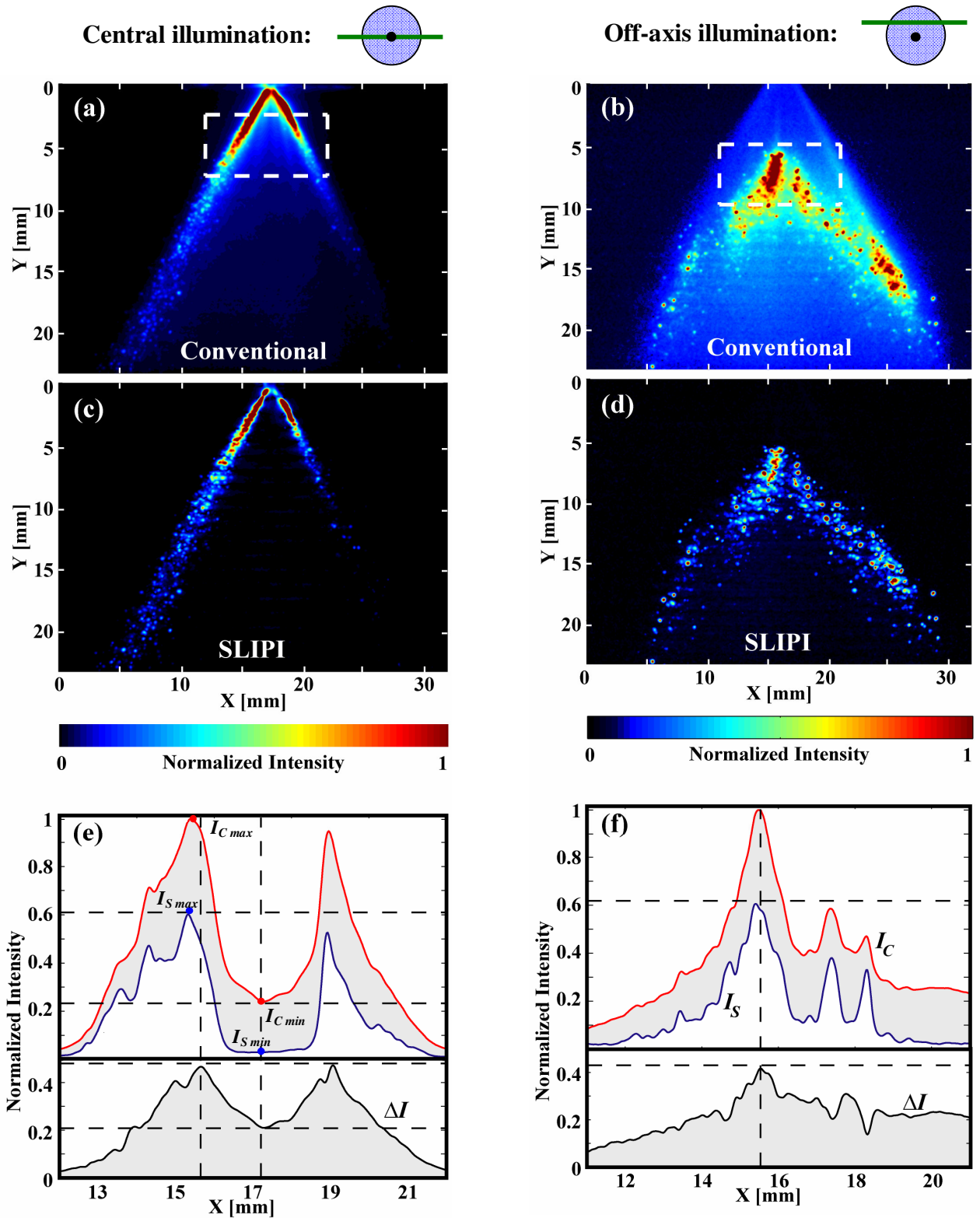


**Fig.4.** Comparison between the conventional planar Mie imaging and SLIPI: Each image corresponds to an average of 50 “single shot” SLIPI images. The laser sheet crossed the centre line of the spray in (a) and (c); whereas, in (b) and (d) the planar illumination was  $\sim 5$ mm off-axis (behind) from the nozzle centre. An intensity profile corresponding to the cross-section, defined within the dashed boxes (of dimension 10 X 5 mm) is shown below the images in (e) and (f). The grey area indicates the contribution from multiple scattering. A maximum value of  $\Delta I = 47\%$  in (e) and of  $\Delta I = 42\%$  in (f) is suppressed in the the conventional image by means of SLIPI.

For the off-axis case, multiple scattering should in one hand increase due to the longer photon mean path within the spray but, in another hand, should decrease since the densest region is no longer illuminated. Finally, this explains the maximum  $\Delta I$  of 42 % seen in (f), which is of the same order to the one previously measured. Once again, the position of the  $I_C$  peak value coincides with the maximum  $\Delta I$ .

When the beam is crossing the spray, losses of light energy occurs along the laser sheet due to extinction. This attenuation of light is apparent in images (a) and (c). Methods to correct these attenuation effects can complementary be applied with SLIPI.

### b) Application to a nebuliser

As mentioned previously, the total time needed to record the three images was equal to 110  $\mu$ s. Since this time delay only allows a flow velocity up to 25 cm/s to be frozen, it is not adequate for single measurements within the hollow-cone spray, where the velocity of the droplets can reach 50 m/s. In this subsection we show that when probing a sufficiently low flow motion, no structure displacement from shot-to-shot can be observed within the three successive recorded images, allowing an accurate “single shot” SLIPI image to be recorded.

The investigated scattering medium was in this case a dilute flow of small water droplets ( $\sim 5 \mu$ m in diameter) created by a nebuliser. A flow of nitrogen was introduced in the center of the nebuliser, in order to create a region where no scattering event occurs. Similar to the previous case, the intensity of the signal detected within this known region should be zero.

In Fig.5 a comparison between the conventional and the SLIPI image is presented. Figure 5 (a) corresponds to the conventional image, while the SLIPI image is shown in (b).

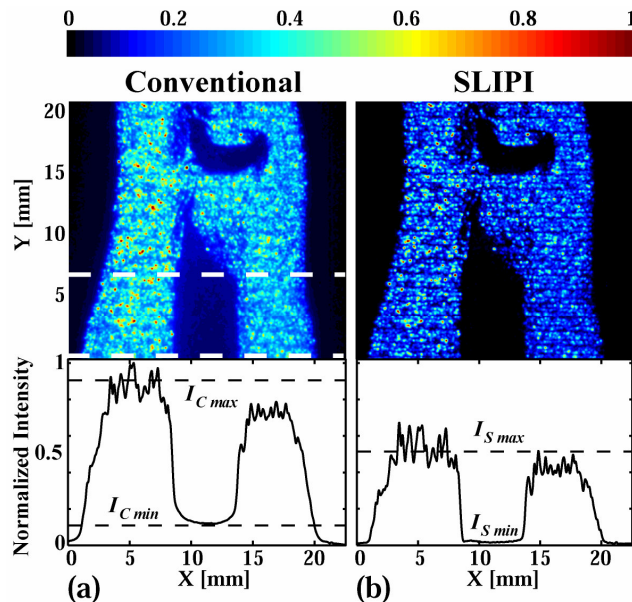


**Fig. 5.** Comparison between conventional planar Mie imaging and SLIPI. In (a) the conventional image is presented, while (b) shows the SLIPI image. Below each image the corresponding cross section, integrated between  $0 \text{ mm} < Y < 6 \text{ mm}$ , is given (see Kristensson *et al.* [12]).

As can be seen, the intensity in the conventional image is higher, since it includes all detected light. Below each image an intensity profile, defined between the dashed lines in Fig. 5 (a), is shown.

In this set of “single shot” images, the contrast increases from  $C = 76 \%$  in the conventional image, to  $C = 95 \%$  for the SLIPI image ( $C$  is evaluated according to Eq.5).

These results, which are fully analysed in [12], demonstrates the capability of SLIPI on a frozen flow motion. To investigate faster flow motions, the time delay from shot to shot must be decreased. One approach is to use a thicker rotating glass plate. Another solution is to use a grating with a higher spatial frequency. Finally, by using three gratings (instead of one) along each beam path, the rotating glass plate could be removed. In this case, the minimum time separation will instead be governed by the camera or the laser system.

## CONCLUSION

In summation, we have presented a novel approach to suppress the multiply scattered light from laser sheet images. The technique (SLIPI) was tested in the dense region of a hollow-cone spray based on a Mie scattering measurement. A multiple scattering contribution of 47 % arising from the dense spray region could be removed. This suppression led to a large improvement in image contrast going from 61 % up to 89 %. It has been also demonstrated that the method applies both for averaged and “single shot” images. Finally, further improvements will focus on the correction of the laser sheet attenuation and on the implementation of the technique for other planar laser based diagnostics such as Planar Laser Induce Fluorescence (PLIF).

## ACKNOWLEDGMENT

The authors wish to show their appreciation to the Linné Center within the Lund Laser Center (LLC) as well as CECOST through SSF and STEM for financial support.

## REFERENCES

- [1] R. J. Adrian “Twenty years of particle image Velocimetry,” *Exp. Fluids* 39 159-69 (2005).
- [2] Maas, H.-G., Grün, A., Papantoniou, D., “Particle Tracking in three dimensional turbulent flows - Part I: Photogrammetric determination of particle coordinates,” *Exp. Fluids*. 15, 133-146 (1993)
- [3] R. J. Bazile and D. Stepowski, “Measurements of vaporized and liquid fuel concentrations in a burning spray jet of acetone using planar laser-induced fluorescence,” *Exp. Fluids* 20, 1-9 (1995).
- [4] R. Domann and Y. Hardalupas, “Quantitative measurement of planar droplet Sauter mean diameter in sprays using planar droplet sizing,” *Part. Part. Syst. Charact.* 20, 209-218 (2003).
- [5] T. Réveillé, A study of fuel injection and mixture formation for gasoline direct injection engine, Cranfield University, 2005.
- [6] A. Serpenguzel, S. Kucuksenel, and R. K. Chang, “Microdroplet identification and size measurement in

- sprays with lasing images,” *Opt. Express* 10, 1118-1132 (2002).
- [7] E. Berrocal, Multiple scattering of light in optical diagnostics of dense sprays and other complex turbid media PhD Thesis, Cranfield University, 2006.
  - [8] R. Abu-Gharbieh, J. L. Persson, M. Forsth, A. Rosen, A. Karlstrom, and T. Gustavsson, “Compensation method for attenuated planar laser images of optically dense sprays,” *Appl. Opt.* 39, 1260-1267 (2000).
  - [9] V. Sick and B. Stojkovic, “Attenuation effects on imaging diagnostics in hollow-cone sprays,” *Appl. Opt.* 40, 2435-2442 (2001).
  - [10] S. E. D. Webb, Y. Gu, S. L  v  que-Fort, J. Siegel, M. J. Cole, K. Dowling, R. Jones, P. M. W. French, M. A. A. Neil, R. Juskaitis, L. O. D. Sucharov, T. Wilson and M. J. Lever, “A wide-field time-domain fluorescence lifetime imaging microscope with optical sectioning”, *Rev. Sci. Instrum.* 73, 1898-1907 (2002).
  - [11] B. Paulsen Husted, Experimental measurements of water mist systems and implications for modelling in CFD, PhD Thesis, Lund University, 2007.
  - [12] E. Kristensson, E. Berrocal, M. Richter, S-G. Pettersson, and M. Ald  n, “Suppression of multiple scattering in planar laser imaging using structured illumination,” Submitted to *Opt. Lett.* (May 2008)